ACS APPLIED MATERIALS & INTERFACES

www.acsami.org

Research Article

# Antifouling Properties of Pluronic and Tetronic Surfactants in Digital Microfluidics

Man Ho, Aaron Au, Robert Flick, Thu V. Vuong, Alexandros A. Sklavounos, Ian Swyer, Christopher M. Yip, and Aaron R. Wheeler*

Cite This: *ACS Appl. Mater. Interfaces* 2023, 15, 6326−6337

Read Online

ACCESS | Metrics & More | Article Recommendations | Supporting Information

**ABSTRACT:** Fouling at liquid−solid interfaces is a pernicious problem for a wide range of applications, including those that are implemented by digital microfluidics (DMF). There are several strategies that have been used to combat surface fouling in DMF, the most common being inclusion of amphiphilic surfactant additives in the droplets to be manipulated. Initial studies relied on Pluronic additives, and more recently, Tetronic additives have been used, which has allowed manipulation of complex samples like serum and whole blood. Here, we report our evaluation of 19 different Pluronic and Tetronic additives, with attempts to determine (1) the difference in antifouling performance between the two families, (2) the structural similarities that predict exceptional antifouling performance, and (3) the mechanism of the antifouling behavior. Our analysis shows that both Pluronic and Tetronic additives with modest molar mass, poly(propylene oxide) (PPO) ≥50 units, poly(ethylene oxide) (PEO) mass percentage ≤50%, and hydrophilic−lipophilic balance (HLB) ca. 13−15 allow for exceptional antifouling performance in DMF. The most promising candidates, P104, P105, and T904, were able to support continuous movement of droplets of serum for more than 2 h, a result (for devices operating in air) previously thought to be out of reach for this technique. Additional results generated using device longevity assays, intrinsic fluorescence measurements, dynamic light scattering, asymmetric flow field flow fractionation, supercritical angle fluorescence microscopy, atomic force microscopy, and quartz crystal microbalance measurements suggest that the best-performing surfactants are more likely to operate by forming a protective layer at the liquid−solid interface than by complexation with proteins. We propose that these results and their implications are an important step forward for the growing community of users of this technique, which may provide guidance in selecting surfactants for manipulating biological matrices for a wide range of applications.

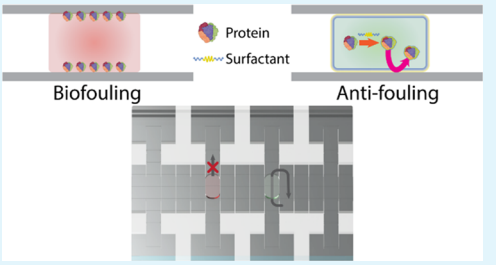


**KEYWORDS:** *digital microfluidics, nonspecific adsorption, fouling, pluronics, tetronics, electrowetting*



## INTRODUCTION

Surface fouling is the (typically unwanted) nonspecific adsorption of biological molecules onto a phase interface. The most important type of fouling is the adsorption of biopolymers, typically proteins, from aqueous media onto a solid surface, a process that is often driven entropically. This phenomenon is a serious problem for a wide range of applications, including implanted medical devices,[1,2] bioreactors,[3] filtration membranes,[4,5] and diagnostic devices.[6,7] Fouling is exacerbated in many of these applications because of a high surface-area-to-volume ratio, and the extent of fouling is often mitigated by coating surfaces with hydrophilic, noncharged polymers, which can attract a tightly bound layer of water molecules that resist the adsorption of proteins when exposed to aqueous media.[6−11]

Digital microfluidics (DMF) is a fluid-handling technique in which nano- to microliter droplets are manipulated by electrostatic forces on an array of insulated electrodes.[12] Because of its capacity to precisely and automatically dispense, mix, merge, and split discrete droplets, DMF is becoming an increasingly popular tool for biological and biochemical applications,[13] including single-cell Omics analysis,[14,15] antibiotic susceptibility testing,[16,17] and diagnostic immunoassays.[18,19] DMF devices typically comprise two substrates with droplets sandwiched between them. All surfaces on these substrates are coated with a fluorinated and hydrophobic polymer (such as Teflon-AF, Fluoropel, or Cytop), to reduce the surface energy for aqueous droplet manipulation. Unfortunately, this requirement precludes the use of the hydrophilic antifouling coatings that are used in other applications,[6−11] making the technique particularly susceptible to fouling. This is a major challenge for DMF, as the unwanted adsorption and accumulation of proteins and other biological molecules on the device surfaces can cause device failure.

There are numerous strategies[20−23] that have been employed to mitigate the effects of fouling in digital microfluidics; none are perfect, and the challenge remains a critical one in the field. The most common strategy has been the inclusion of amphiphilic poloxamer (trade name Pluronic) additives in aqueous solutions

Received: September 25, 2022
Accepted: January 11, 2023
Published: January 25, 2023

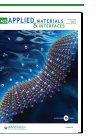





https://doi.org/10.1021/acsami.2c17317
*ACS Appl. Mater. Interfaces* 2023, 15, 6326−6337

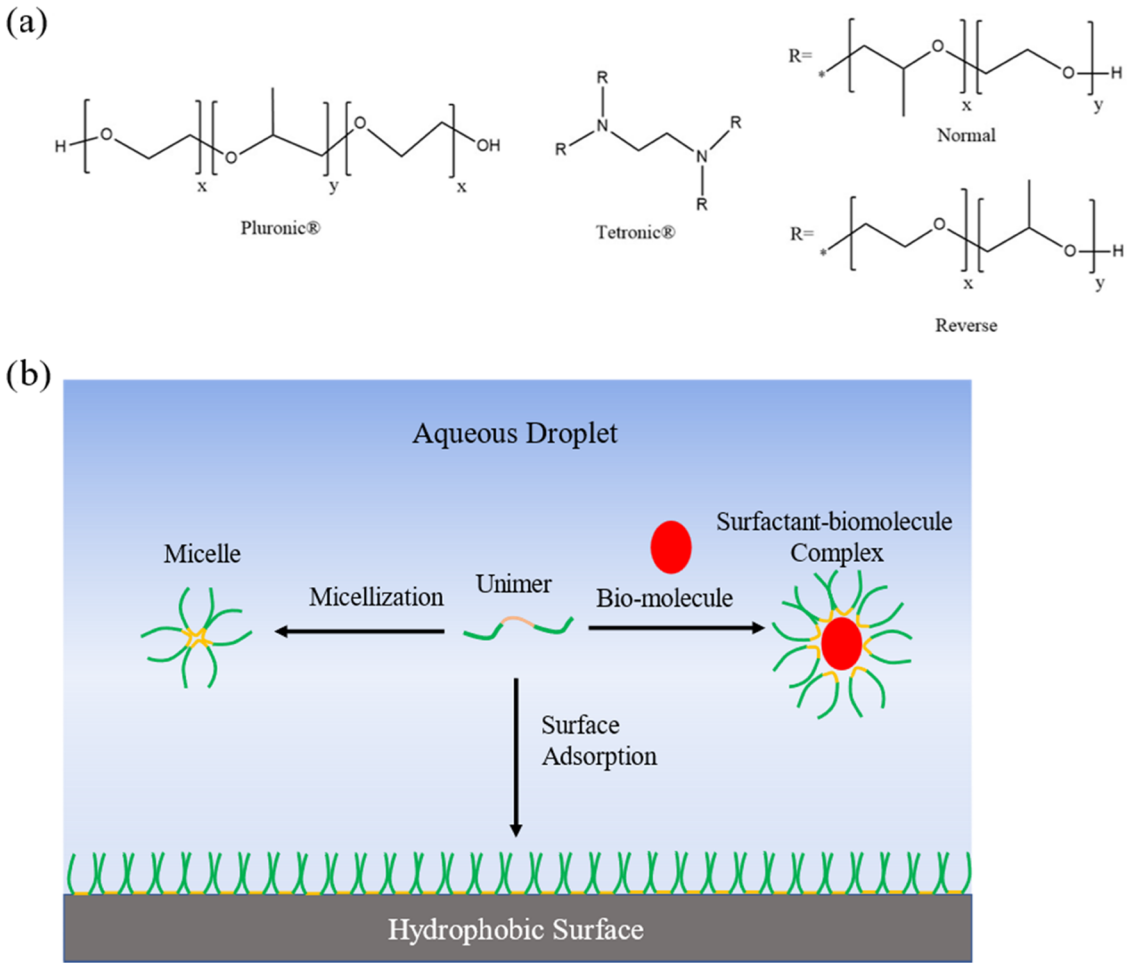


**Figure 1.** Surfactant additives to reduce fouling in digital microfluidics. (a) Structures of Pluronic[41] and Tetronic[42] surfactants, illustrating the R-groups for "normal" and "reverse" forms of the latter. (b) Schematic illustrating the potential processes involved in surfactant-mediation of fouling in DMF devices. As shown, surfactant unimer, shown with hydrophobic cores (orange) and hydrophilic tails (green) similar to the structure of Pluronic, may self-aggregate to form micelles or complex with biomolecules (red ovals) or adsorb to the interface between the droplet and the hydrophobic device surface.

to enable manipulation of droplets. Pluronics are block copolymers that feature two hydrophilic poly(ethylene oxide) (PEO) chains flanking a hydrophobic poly(propylene oxide) (PPO) core, as shown in Figure 1a. In particular, Pluronic F68 was reported to be useful in reducing fouling in DMF devices from dilute protein solutions more than a decade ago.[24,25] Since that time, this strategy has been employed in research reports[26−36] from groups all over the world for a wide range of applications of DMF.

A more recent trend is the use of poloxamines as antifouling additives in DMF. These substances, which are sold under trade name Tetronic, also feature block copolymer chains of PEO and PPO, but in the shape of an "X" around an ethylene diamine core. As shown in Figure 1a, in normal configuration, the PEO block is on the outside with the PPO block in the center (like Pluronics), but in the reverse configuration, the PPO block is on the outside of the molecule. In particular, the reverse-configured Tetronic 90R4 (T90R4) has been shown to allow manipulation of whole blood, serum, cell lysates, and other high protein content solutions in DMF devices.[37−40] These applications were historically not possible for DMF devices operated with aqueous droplets suspended in air; thus, T90R4 has been a "game-changer" for the DMF community, enabling interesting new applications such as the operation of portable serological assays in pin-prick/blood samples in remote field trials.[38]

The discovery of the unique properties of T90R4 in the context of the general utility of block copolymers of PEO and PPO for DMF raises important questions about their antifouling effects, including: (1) Is the exceptionally powerful antifouling property unique to Tetronic 90R4 (perhaps related to its reverse structure) or to the Tetronic family at large? and (2) What are the structural and physical properties shared between surfactants with outstanding antifouling performance? Here, we describe our work evaluating 19 different Pluronic and Tetronic formulations based on their abilities to enable actuation of serum (i.e., the viscous, protein-rich solution that remains after clotting whole blood) in DMF. Surfactant additives enabling long-term actuation of this sample were identified, and their physical and structural properties were examined.

In this paper, we also present our findings related to a third question: (3) What are the mechanisms of the reduction in biomolecule adsorption for poloxamer and poloxamine additives? Here, we considered two general hypotheses, as illustrated in Figure 1b. In hypothesis (i), surfactant unimers are thought to reduce protein adsorption to device surfaces by directly interacting with proteins[43,44] (either in complexes or micelles), reducing their affinity to the surface. In hypothesis


https://doi.org/10.1021/acsami.2c17317
ACS Appl. Mater. Interfaces 2023, 15, 6326−6337

(ii), surfactant unimers are thought to reduce protein adsorption to device surfaces by forming a contiguous, adsorbed layer at the interface between droplet and hydrophobic device surfaces, thus shielding the surface from proteins. To test these hypotheses, a sample matrix containing bovine serum albumin (BSA) with surfactant additives was characterized by various techniques to evaluate plausible antifouling mechanisms. We propose that the results of this study are intriguing and instructive, laying the groundwork for the selection of surfactant additives for a wide range of applications for digital microfluidics, going forward.

## EXPERIMENTAL SECTION

**Reagents and Materials.** Unless specified otherwise, reagents were purchased from Sigma-Aldrich (Oakville, Canada). Pluronics and Tetronics (BASF Corp., Germany) were generously donated by BASF Corporation (Wyandotte). Parylene-C dimer was from Specialty Coating Systems (Indianapolis), and Teflon-AF 1600 was from DuPont (Wilmington). PFC110 fluorinated solvent was purchased from Cytonix (Beltville). Fatty-acid free reagent grade bovine serum albumin was purchased from Proliant Biologicals (Ankeny). Gibco fetal bovine serum was purchased from Thermo Fisher (Mississauga, Canada). Poly(ethylene glycol) 8000 (PEG 8000) was purchased from BioShop (Burlington, Canada). Stock solutions of bovine serum albumin (BSA), Pluronics, and Tetronics were prepared in Dulbecco's phosphate-buffered saline (DPBS) at 80 g/L and 10% wt/wt, respectively. Stock protein solutions and Pluronic L92 were stored at 4 °C until use; others were kept at room temperature.

**DMF Device Fabrication and Operation.** Digital microfluidic devices were formed from bottom and top plates. Most bottom plates were formed by inkjet printing silver electrodes on a Novele printing media (Novacentrix, Austin) as detailed elsewhere.[45] Briefly, a device design (described previously[46]) was created using AutoCAD and Inkscape and was then printed using an Epson C88+ printer (Markham, Canada), followed by drying overnight at room temperature. The printed sheets were then coated by chemical vapor deposition with a layer of parylene-C (~6 $\mu$m thick) and spin-coated with Teflon-AF 1600 (~44 nm thick) from a 1% solution in PFC110 at 2000 rpm for 30 s. For some experiments, bottom plates with a similar design were formed from glass patterned with chromium electrodes (and coated with parylene-C and Teflon-AF as above) as described elsewhere.[37] Top plates were prepared by forming spin-coated layers of Teflon-AF 1600 with the same parameters (~44 nm thick) on indium tin oxide (ITO)-coated glass slides (25 mm × 75 mm) (Delta Technologies, Loveland). Two layers of double-sided tape (3M Company, Maplewood) were used as spacers (~180 $\mu$m) between top and bottom plates. DMF devices were interfaced *via* pogo-pin connector to the open-source DropBot Control system (http://microfluidics.utoronto.ca/dropbot/) and droplet movement (driven by applying sine-wave voltage traces of 87−95 $V_{RMS}$ or 25 $\mu$N/mm$^2$ at 10 kHz, conditions found to be below the saturation forces[46] for all liquids tested) was programmed by MicroDrop software as described previously.[46,47]

**Device Longevity Assays.** A device longevity assay protocol was adapted from previous work,[46] in which droplets were automatically actuated back and forth between a pair of electrodes while monitoring droplet position and velocity by measuring the capacitance. Each step comprised the application of actuation voltage for 8 s, and the number of steps was set at 75, 150, or 900 for 10 min, 20 min, or 2 h experiments, respectively. Each condition was evaluated in three replicate 4.3 $\mu$L droplets. Each actuation step was deemed successful for droplets that moved onto the actuated electrode (4 mm) within 8 s with an average velocity (the 'threshold') of at least 0.5 mm/s. In experiments with serum samples, 13 Pluronic (L35, F38, L44, L62, L64, F68, F88, L92, P104, P105, F108, P123, and F127) and 6 Tetronic (T304, T904, T90R4, T908, T1107, and T1304) surfactants were evaluated at four concentrations: 0.5×, 1×, and 2× the critical micelle concentrations (CMCs) reported in the literature, and at 0.1% wt/wt, all in 90% FBS v/v in DPBS for 20 min. (F38 and T1304 do not have literature CMC values and therefore, the concentrations tested were 0.1, 0.5, 1, and 2% wt/wt.) In 2 h experiments with fetal bovine serum, a subset of four surfactants. P104, P105, T904, and T90R4 were each evaluated at 0.1% wt/wt in samples containing 90% v/v FBS in DPBS. Finally, in experiments with samples containing BSA, three Pluronic (F68, P104, P105) and two Tetronic (T904 and T90R4) surfactants were each evaluated for 10 min windows at concentrations ranging from 0.0001 to 1.0% wt/wt [except for F68 (0.0001−2.0% wt/wt)] (with at least 4 concentrations per surfactant) in DPBS containing 0.40, 4.0, and 40 mg/mL BSA. In these experiments, the lowest concentration of surfactant was recorded that enabled successful completion of 75 steps at the velocity threshold indicated above. During device longevity assay, all reservoirs were filled (and repeatedly refilled) with DPBS to reduce evaporation.

**Critical Micelle Concentration Measurements.** A stock solution of pyrene (100 $\mu$M) was prepared in acetone. In each experiment, 10 $\mu$L of the stock pyrene solution was pipetted into a 2 mL centrifuge tube and allowed to dry in the fume hood for 15 min. An aliquot (1 mL) of surfactant solution with concentration between 0.001 and 4.0% wt/wt in DPBS was added to each tube, which was agitated in a rotatory mixer overnight; 300 $\mu$L aliquots of the surfactant solution were then transferred to wells in a Falcon 96-well black bottom well plate. The fluorescence intensities in each well were measured on an Infinite M200 pro monochromator plate reader (Tecan, Crailsheim, Germany) with excitation at 335 nm (9 nm bandwidth) and emission at 380 nm (20 nm bandwidth) at 23 °C, with gain and number of flashes set at 107 and 25, respectively. The average fluorescence was plotted as a function of surfactant concentration, and the critical micelle concentration was determined from the intercept of two lines of regression. The first line was fitted to the average fluorescence intensities from the lowest 4 to 6 concentrations (the actual number of concentrations was determined from regressing successive number of data points until yielding a maximum $R^2$ value). The second line was fitted to the average fluorescence intensities from the highest three concentrations.

**Dynamic Light Scattering (DLS) and Asymmetric Flow Field Flow Fractionation ($AF_4$).** Solutions of BSA and one of the surfactants in DPBS were prepared such that the final concentrations were 4 mg/mL (BSA) and 0.01% wt/wt (P104, P105, T904, T90R4), 0.1% wt/wt (F68) or 8 mM (sodium dodecyl sulfate, SDS), respectively. For DLS analysis, a 1 mL aliquot of BSA/surfactant mixture was pipetted into a 1.5 mL semi-micro disposable cuvette (BrandTech, Wertheim, Germany) and was evaluated in a Zetasizer Nano S (Malvern Panalytical, Malvern, U.K.), with refractive index of sample material (RI) and absorption coefficient ($k$) set to 1.45 and 0.001, respectively. Data collection and analysis were completed by the companion Zetasizer software (Version 8.01) using the "protein analysis" model.

For $AF_4$ analysis, solutions of BSA/surfactant mixtures were separated using Wyatt Eclipse DualTec FFF (Wyatt Technology, Santa Barbara) equipped with a short channel, a 10 kDa regenerated cellulose membrane, and a 350 $\mu$m wide channel spacer. Briefly, 60 $\mu$L of sample was injected and eluted from the short channel using 1× PBS as the mobile phase. The system was operated with a detector flow of 1 mL/min and a focus flow of 1.5 mL/min. The separation was done in six steps: (1) elution mode (1 min, cross-flow $V_x$ = 3 mL/min), (2) focus mode (1 min, $V_x$ = 0 mL/min), (3) focus + inject mode (1 min, $V_x$ = 0 mL/min), (4) focus mode (2 min, $V_x$ = 0 mL/min), (5) elution mode (20 min, $V_x$ = 3 mL/min), (6) focus + inject mode (5 min, $V_x$ = 0 mL/min). The detectors comprised a UV absorbance detector (Agilent 1260 Infinity VWD) operated at 250 nm, a RI detector (Wyatt Optilab T-rEX), and a multiangle light scattering detector (Wyatt Dawn Helios II). Data collection and processing were programmed using the companion software, Wyatt Astra 6.1, using the "DEBEYE" light scattering model.

**Intrinsic Tryptophan Fluorescence Measurements.** Solutions of BSA and one of the subset surfactants in DPBS were prepared such that the final concentrations were 4 mg/mL (BSA) and 0.01% wt/wt (P104, P105, T904, T90R4) or 0.1% wt/wt (F68), respectively. A 1 mL aliquot was pipetted into a disposable fluorimeter cuvette (759115, Brand, Wertheim, Germany), and fluorescence spectra were collected using a FluoroMax-3 Spectrofluorometer (Horiba, Kyoto, Japan) at


https://doi.org/10.1021/acsami.2c17317
ACS Appl. Mater. Interfaces 2023, 15, 6326−6337

**Table 1. Physical Properties of the Pluronic and Tetronic Surfactants Used in This Study**

| surfactant | average molecular weight (g/mol)[a] | ave. PPO chain length (n)[b] | ave. PEO chain length (m)[b] | % PEO content[a] | hydrophilic−lipophilic balance (HLB)[a] | literature CMC value used for screening (% wt/wt)[a,b] | experimental CMC value[c] (% wt/wt) at 23 °C in DPBS |
|---|---|---|---|---|---|---|---|
| | | | | Pluronic | | | |
| L35 | 1900 | 16.4 | 21.6 | 50 | 19 | 1.0 | |
| F38 | 4700 | 15.9 | 83.6 | 80 | 31 | | |
| L44 | 2200 | 22.8 | 20.0 | 40 | 16 | 0.79 | |
| L62 | 2500 | 34.5 | 11.4 | 20 | 7 | 0.10 | 1.7 |
| L64 | 2900 | 30 | 26.4 | 40 | 15 | 0.14 | 1.6 |
| F68 | 8400 | 29.0 | 152.7 | 80 | 29 | 0.40 | 1.0 |
| F88 | 11,400 | 39.3 | 207.3 | 80 | 28 | 0.29 | |
| L92 | 3650 | 50.3 | 16.6 | 20 | 6 | 0.032 | |
| P104 | 5900 | 61.0 | 53.6 | 40 | 13 | 0.0010 | 0.43 |
| P105 | 6500 | 56.0 | 73.9 | 50 | 15 | 0.0040 | 0.47 |
| F108 | 14,600 | 50.3 | 265.5 | 80 | 27 | 0.032 | 0.69 |
| P123 | 5750 | 69.4 | 39.2 | 30 | 8 | 0.0025 | |
| F127 | 12,600 | 65.2 | 200.5 | 70 | 22 | 0.0035 | |
| | | | | Tetronic and Tetronic Reverse | | | |
| T304 | 1650 | 17.1 | 15.0 | 40 | 16 | 1.00 | |
| T904 | 6700 | 69.3 | 60.9 | 40 | 15 | 0.70 | 1.1 |
| T90R4 | 7200 | 72 | 64 | 40 | 7 | 0.014 | 1.0 |
| T908 | 25,000 | 86.2 | 454.5 | 80 | 31 | 1.00 | |
| T1107 | 15,000 | 77.6 | 238.6 | 70 | 24 | 0.70 | |
| T1304 | 10,500 | 108.4 | 96.4 | 40 | 14 | | |

[a]Provided by manufacturer and suppliers, BASF Corp. and Sigma-Aldrich. [b]Data adapted from the literature[53−56] without solvent specified and at 37 °C. [c]Data generated here using a modified thin-film rehydration method.[57]

room temperature (25 °C) in the range of 310−410 nm (in 5 nm intervals) with excitation wavelength at 280 nm. A control sample of BSA was prepared and analyzed identically but with 8 mM SDS in DPBS. In each case, spectra were collected from blanks (surfactants in buffer and buffer only) under the same conditions and subtracted from the sample spectra.

**Fluorescent Labeling, Purification, and Quantification of Surfactants.** Three surfactants (F68, P105, and T904) were fluorescently conjugated with 5-(4,6-dichlorotriazinyl)-aminofluorescein (5-DTAF) using a modification of the procedure described in Ahmed et al.[48] Briefly, 10% wt/wt stock surfactant solutions were prepared in 0.1 M sodium bicarbonate solution at pH 9.5, and a stock solution of 20 g/L (40 mM) 5-DTAF was prepared in DMSO. Each stock surfactant solution was further diluted in 0.1 M sodium bicarbonate to 90% of its experimentally determined CMC (Table 1) and mixed with an appropriate volume of the 5-DTAF stock solution such that the molar ratio of 5-DTAF to surfactant was 4:1. The reaction mixtures were incubated at room temperature on a rotatory mixer overnight. The reaction products were then purified using a PD minitrap G-25 spin protein purification column (Cytiva, Marlborough). Each 5-DTAF conjugated surfactant solution was purified three times in succession according to the protocol provided by the manufacturer, using DPBS to condition the columns and elute the surfactants.

The concentrations of purified 5-DTAF conjugated surfactants were determined using a colorimetric assay described by Ghebeh et al.[49] First, calibration standards of underivatized F68, P105, and T904 were prepared by dissolving surfactants in DPBS with concentrations of 0.00, 0.01, 0.05, 0.08, 0.10, 0.15, and 0.20% wt/wt. A 200 μL aliquot of each surfactant standard was mixed with 100 μL of cobalt thiocyanate solution (3 g of cobalt nitrate and 20 g of ammonium thiocyanate in 100 mL of water), 80 μL of ethanol, and 200 μL of ethyl acetate. The mixture was then centrifuged at 10,000 rpm for 2 min, forming a blue pellet at the bottom of the tube. The supernatant was decanted away, and the blue pellet was washed with multiple 200 μL aliquots of ethyl acetate until the supernatant became colorless. The washed pellet was redissolved in 1 mL of ice-cold acetone, and 300 μL aliquots of this light-blue solution were transferred to wells in a Falcon 96-well black bottom well plate. The well plate was kept on ice to minimize evaporation until loading on a well-plate reader. Absorbance measurements at 623 nm were collected on an Infinite M200 Pro monochromator plate reader with temperature, bandwidth, and number of flashes set to 23 °C, 9 nm, and 25 nm, respectively. All measurements were made in triplicate, and average blank absorbance (from 300 μL aliquots of neat acetone) was subtracted from the average sample absorbances to yield corrected absorbances. These data were then plotted as a function of surfactant concentration to establish calibration curves for underivatized F68, P105, and T904. Once the calibration curves were established, the assay was repeated with purified 5-DTAF conjugated surfactants, comparing their corrected absorbance values to the calibration curves to determine their concentrations.

The conjugation efficiency for modifying surfactants with 5-DTAF was determined by absorbance. Briefly, a series of calibration standards of 5-DTAF with concentrations ranging from 0.0001 to 0.1000 mM was prepared by diluting 40 mM stock 5-DTAF solution in DPBS. Next, 400 μL aliquots of each of the 5-DTAF standards and each of the purified 5-DTAF conjugated surfactant solutions were transferred to wells in a Falcon 96-well black bottom well plate. Absorbance measurements at 498 nm were collected on an Infinite M200 Pro monochromator plate reader with temperature, bandwidth, and number of flashes set to 23 °C, 9 nm, and 25 nm, respectively. All measurements were made in triplicate, and the average blank absorbance (from 400 μL aliquots of DPBS) was subtracted from the average sample absorbances to yield corrected absorbances. The corrected absorbances from the 5-DTAF standards were plotted as a function of 5-DTAF concentrations to establish a calibration curve. Finally, the concentrations of 5-DTAF fluorophores found in the conjugated surfactant solutions were determined by comparing the corrected absorbances of those solutions to the calibration curve.

**Supercritical Angle Fluorescence (SAF) Microscopy Measurements.** No. 1 22 × 22 mm micro-cover glasses (VWR International, Mississauga, Canada) were spin-coated with 0.5% wt/wt Teflon-AF 1600 in FC-40 at 3000 rpm for 30 s. The coated cover glasses were baked at ∼170 °C on a hot plate for 15 min. The average thicknesses of the Teflon layers were determined to be 7.66 ± 0.48 nm using a Bruker Resolve atomic force microscope (AFM, Massachusetts) with an SNL-D probe. Three fluorescently labeled surfactants (F68, P105, and T904) were diluted to 0.1% wt/wt in DPBS, and in 40 mg/mL BSA in DPBS. Separate control solutions of 30 μM fluorescein were


https://doi.org/10.1021/acsami.2c17317
ACS Appl. Mater. Interfaces 2023, 15, 6326−6337

also formed in DPBS containing unlabeled F68, P105, and T904 (also at 0.1% wt/wt) with and without 40 mg/mL BSA.

Supercritical angle fluorescence (SAF) microscopy measurements were made using a custom modular platform built around an IX-83 inverted microscope body (Olympus, Japan), as described in detail elsewhere.[50] Briefly, a 488 nm laser was passed through a spatial filter featuring an annulus (7.38 mm inner diameter and 8.25 mm outer diameter), and the image of the annulus was projected into the back focal plane of a high NA 100× objective (UApoN 100×/RI 1.49 oil, Olympus, Japan). Emission was collected by the same objective and projected through a tube lens onto the camera. Images were collected using a Prime BSI sCMOS camera (Photometrics, Arizona) using micromanager[51,52] in 16-bit HDR mode. Images were processed using an automated python script [https://github.com/YipLab/IX83-Modules/tree/master/SAF] relying on a Hough's Circle Transform to identify the SAF ring as described previously.[50] Briefly, the ring was typically found at around 325 pixels from the center, and the intensities of pixels 0−324 and 325−351 along the radius were averaged and recorded as the "subcritical fluorescence signal" and the "SAF signal," respectively. In each experiment, a Teflon-AF-coated cover glass was aligned relative to the 100× objective (with the noncoated side facing the objective) with a few drops of type-F immersion oil (Olympus, Canada) between the lens and the cover glass. For labeled surfactant samples, a 20 $\mu$L droplet of sample was pipetted onto the Teflon-coated side and allowed to equilibrate for 2 min. The objective was focused on the solid−liquid interface, the 488 nm laser source was engaged and a SAF image was acquired from the droplet with exposure time set at 250 ms. For control (fluorescein) solutions, an additional intensity adjustment step was applied prior to image acquisition. In brief, the 488 nm laser intensity was adjusted using a linear polarizer (LPVISE100-A, Thorlabs) to match the subcritical intensity of each control to its respective labeled surfactant sample. Each sample and control were evaluated five times (in five different droplets), and the mean SAF intensities were computed by averaging the SAF intensity of individual image.

**Atomic Force Microscopy.** Teflon-AF-coated cover glasses were prepared as described above (for SAF microscopy) and were assembled in a live cell chamber (A7816, Thermo Fisher, Canada). A 1000 $\mu$L aliquot of PBS or PBS with 0.1% w/w F68 or T904 was loaded into the chamber. The chamber was then placed into an ultrasonic bath for 2 min, followed by an 8 min incubation. The micro-cover glass was then scanned by tapping-mode AFM (Bruker, Resolve) using a Bruker Resolve atomic force microscope (Massachusetts) with a sharp AFM tip (SNL-10-A). The frequency of tapping was tuned to the highest peak between 10 and 50 kHz. After engaging the tip, a 5 $\mu$m × 5 $\mu$m image of the surface was acquired as a 512 × 512 points dataset at a scan rate of 0.25 Hz. Each image took approximately 35 min to acquire. The data were processed using version 1.90 of the Nanoscope Analysis software. Images were first flattened to the second degree to remove bowing and then filtered using a 3 × 3 median filter.

**Quartz Crystal Microbalance with Dissipation (QCM-D) Measurements.** Quartz crystal microbalance with dissipation (QCM-D) measurements was acquired using gold sensors (QSX 301, Biolin Scientific, Sweden) that had been spin-coated with 0.5% wt/wt Teflon-AF 1600 in FC-40 at 3000 rpm for 30 s. In each experiment, a coated sensor was loaded into a QSense Analyzer system (QSense E4, Biolin Scientific, Sweden) equipped with QSoft software, operating at constant flow rate (0.1 mL/min) and temperature (23 °C). After equilibration in PBS, the sample (PBS, PBS containing surfactant, or PEG 8000 at 0.001% wt/wt) was pumped over the sensor until the signals were stable (i.e., when the frequency shift changed less than 1 Hz in 10 min). Finally, PBS was pumped over the sensor to remove any unbound solutes. The viscoelastic properties of adlayer surfactants were analyzed using the Voigt model. The frequency shifts of the sensors ($\Delta f$) and the dissipation energy shifts ($\Delta D$) were used to calculate the total mass of adlayer surfactants using Dfind analysis software (Biolin Scientific, Sweden).

**Replicates and Variance.** All quantitative data are reported as the average values for at least $n = 3$ replicates per condition, with error bars plotted as ± 1 standard deviation of the mean.

## RESULTS AND DISCUSSION

**Pluronic/Tetronic Droplet Additives for DMF Longevity.** This study was designed to probe the properties of Pluronic and Tetronic surfactants, which are block copolymers of the relatively hydrophilic PEO and hydrophobic PPO (Figure 1a). When included as droplet additives in digital microfluidics, these substances exhibit remarkable antifouling behavior (Figure 1b). Nineteen such surfactants (Table 1) were selected on the basis of attainability, spanning a wide range of molecular weights (1900−25,000 g/mol), length of PPO (16−108 units), and mass percentage of PEO (20−80%).

The primary tool used here was a DMF "longevity assay" in which droplets are continuously translated on a device to measure their velocity as a function of time. This kind of analysis has been described previously,[22,24,58,59] but (i) without adequate control for actuation conditions and (ii) for limited durations. To clarify the former—device longevity is dramatically affected by fouling (the effect under investigation here), but also by other phenomena that are unrelated to fouling, including localized dielectric breakdown and/or satellite droplet ejection, known as "velocity saturation effects".[46] If the two types of phenomena (fouling vs saturation effects) are not carefully controlled, the device longevity data may not be a reliable indicator of the effects of fouling. Thus, for the data included here, we have (for the first time to our knowledge) controlled for potential velocity saturation effects. Specifically, force−velocity curves[46] (used to determine the saturation force for each fluid) were collected for all surfactant solutions evaluated here, and care was taken to use subsaturation-force conditions in all longevity assays. (Representative force−velocity curves are shown in Figure S1.) To clarify the latter, the reports that have been published to date[22,24,58,59] have only evaluated droplet movement longevity for a few minutes or less, without (in some cases) reporting that time and evaporation were carefully controlled. Here, we evaluated several controlled times for longevity assays for 20 min and 2 h with measures (filling all reservoirs with aqueous buffer to saturate the atmosphere) to mitigate evaporation, to reflect the boundaries of what might be required for the diverse applications that make use of DMF.

Video clips and representative data from 20 min device longevity assays are shown in Movie S1 and Figure 2—one droplet is completely immobile (representing immediate, catastrophic fouling), another droplet starts moving but then slows until it ceases to move (representing an unacceptably high fouling rate), and a third droplet is mobile throughout the entire experiment (representing an acceptable fouling rate). In typical experiments, these data were scored as a function of number of movement steps completed within a particular velocity threshold. For the experiment represented in Figure 2 that followed 150 programmed steps, the droplets completed 150, 28, and 0 steps, corresponding to normalized longevity scores of 1.00, 0.19, and 0.00, respectively.

As a first test, samples containing 90% v/v fetal bovine serum (FBS) were formed containing a dilution series of each of the 19 surfactants and were subjected to longevity assays. The raw data for these tests are shown in Table S1. An obvious initial finding from these data is that the presence of micelles does not have a strong effect on serum droplet movement. That is—most surfactants either did or did not permit serum droplet movement, regardless of whether the concentration of surfactant was above or below the critical micelle concentrations reported in the literature (Table 1, column 7) or in new measurements



https://doi.org/10.1021/acsami.2c17317
ACS Appl. Mater. Interfaces 2023, 15, 6326−6337

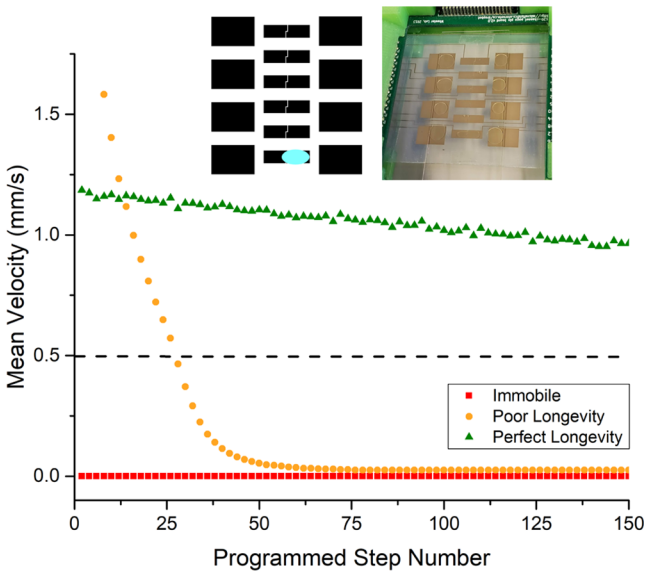


**Figure 2.** DMF longevity assay. Main: representative plots of droplet velocity as a function of programmed step number for a fluid that is immobile (fetal bovine serum, red squares), a fluid with poor longevity (fetal bovine serum with 2.0% wt/wt L62, orange circles), and a fluid with perfect longevity (fetal bovine serum with 0.35% wt/wt T904, green triangles). In each case, the droplets were programmed to move continuously for 150 steps corresponding to a total actuation time of 20 min. The horizontal dashed line at 0.5 mm/s represents the velocity threshold for this (and all) longevity experiment(s), illustrating how the droplets were scored as completing 0, 28, and 150 steps, respectively. Inset: cartoon (left) and photograph (right) of a droplet in a DMF longevity assay.

reported here (Table 1, column 8, Figure S2). However, upon closer inspection of the data, other interesting trends were apparent.

A summary of the results in Table S1 is shown as a heat map in Figure 3. As described in the introduction, surfactant T90R4 was expected to perform well in this test, which was observed here, in the center of Figure 3. Somewhat surprisingly, a cluster of other surfactants was also found to allow for perfect droplet movement of this problematic fluid. This cluster of high-performing additives has an intermediate molecular weight (centered around ~7000 g/mol), a low mass percentage of PEO (≤50%), and a long PPO length (≥50 units). To reiterate, the results in Figure 3 are quite remarkable, illustrating how some of the surfactants that have been used the most in DMF (including F68) do not permit movement of serum, at all, while others that have never been used before in DMF (including T1304) allow for perfect actuation of this sticky, protein-rich liquid. The discovery of this cluster of surfactants that may be useful for these purposes is likely to be important for the field.

We then turned our attention to long-duration (2 h) longevity assays. This period is likely to be "overkill" for many experiments, representing the extreme of what might be needed for select applications. In these tests, a subset of surfactants that resulted in perfect mobility in the original screening study (P104, P105, T904, and T90R4) were evaluated, again on the basis of DMF device longevity for 90% v/v FBS. The results are summarized in Figure 4, which are surprising for a number of reasons. First, we were skeptical that any additives could allow for the extreme condition of serum droplets moving continuously between two electrodes for 2 h; the finding that three additives allowed this to occur is surprising. Second, of the four that were tested, the surfactant that has recently been the most popular in DMF, T90R4, exhibited the worst long-term longevity, with an average longevity score of 0.38 ± 0.06 (46 ± 7.2 min). In contrast, P104, P105, and T904 all exhibited perfect longevity for the duration of the experiment. In considering these remarkable results, we note that P104, P105, and T904 have a hydrophilic−lipophilic balance (HLB) of 13−15, which indicates high water-solubility and capability to stabilize oil-in-water emulsions. In contrast, T90R4 has an HLB of 7. More study is needed, but it seems likely that HLB is a key parameter to consider in future studies.

The findings described above suggest potential answers to questions (1) and (2) from the introduction. First, it seems likely that the reverse structure of T90R4 is not necessary for the reduction of fouling in DMF. In addition, the X-shaped Tetronic structure does not define this trait, either, as several candidates from both the Pluronic and Tetronic family perform similarly. Finally, it seems that some combination of modest molecular weight, low mass percentage of PEO (≤50%), long PPO length (≥50 units), and an HLB of 13−15 may be useful to consider in future studies. Of course, there are other factors that might be considered for different applications, including effects on cell culture and viability, interference with detection and analysis, or the capacity to dispense cleanly in DMF (without forming long droplet "tails"). But it is remarkable to see that serum, a liquid that was formerly out of reach for DMF experiments (operated in air) because of catastrophic fouling, can be manipulated continuously on DMF devices for hours at a time, with the selection of an appropriate Pluronic or Tetronic additive.

**Antifouling Mechanism of Pluronic/Tetronic Additives in Digital Microfluidics.** After evaluating the relationship between surfactant properties and DMF longevity experiments, we turned our attention to question (3) from the introduction—the mechanism of Pluronic and Tetronic antifouling phenomena in digital microfluidics. As proposed in the introduction (Figure 1b), surfactants can prevent surface adsorption of biomolecules through two primary mechanisms,[9,43,60,61] (i) complexation with proteins in solution, or (ii) adsorption to the device surface to form a protective layer. Here, we focused our investigation on solutions of the standard protein bovine serum albumin (BSA) upon mixing with a subset of model Pluronic and Tetronic additives: F68, P104, P105, T904, T90R4. This system was evaluated by identifying minimum surfactant concentration required for DMF actuation, making orthogonal measurements of surfactant/protein complexation, and making orthogonal measurements of labeled and label-free surfactant adsorption on fluoropolymer-coated surfaces.

As a first test for the antifouling mechanism of Pluronic/Tetronic surfactant additives in DMF, we returned to the longevity assay. In DMF, BSA solutions have poor device longevity, but this can be mitigated by the inclusion of surfactant additives. In the case of hypothesis (i), in which surfactant complexation with BSA[62,63] prevents fouling, we would expect that the minimum surfactant concentration required for high-longevity droplet movement would scale with BSA concentration (i.e., more protein molecules require more surfactant molecules to stabilize them). In the case of hypothesis (ii), in which surfactant adsorbed to the solid−liquid (fluoropolymer-surfactant solution) interface[9] prevents fouling, we would expect the minimum surfactant concentration to be independent of BSA concentration. To probe for these effects, a matrix of sixty combinations of BSA and surfactant (three concentrations of


https://doi.org/10.1021/acsami.2c17317
ACS Appl. Mater. Interfaces 2023, 15, 6326−6337

| Average PPO Length | %PEO | | | | | |
|---|---|---|---|---|---|---|
| | 20% | 30% | 40% | 50% | 70% | 80% |
| 15.9 | | | | | | F38 (0.00) |
| 16.4 | | | | L35 (0.00) | | |
| 17.1 | | | T304 (0.00) | | | |
| 22.8 | | | L44 (0.05) | | | |
| 29.0 | | | | | | F68 (0.00) |
| 30.0 | | | L64 (0.76) | | | |
| 34.5 | L62 (0.22) | | | | | |
| 39.3 | | | | | | F88 (0.00) |
| 50.3 | L92 (1.00) | | | | | F108 (0.00) |
| 56.0 | | | | P105 (1.00) | | |
| 61.0 | | | P104 (1.00) | | | |
| 65.2 | | | | | F127 (0.00) | |
| 69.3 | | | T904 (1.00) | | | |
| 69.4 | | P123 (0.53) | | | | |
| 72.0 | | | T90R4 (1.00) | | | |
| 77.6 | | | | | T1107 (0.23) | |
| 86.2 | | | | | | T908 (0.00) |
| 108.4 | | | T1304 (1.00) | | | |

**Figure 3.** Longevity assay—initial screen results. Summary of 20 min device longevity assay results for 90% v/v fetal bovine serum in DPBS. Samples were mixed with one of 19 different surfactants at various concentrations (complete results in Table S1). The best results for each surfactant are plotted as a heat map of normalized longevity score from red (zero longevity) to yellow (poor longevity) and green (perfect longevity) as a function of PPO length (rows) and PEO% (columns).

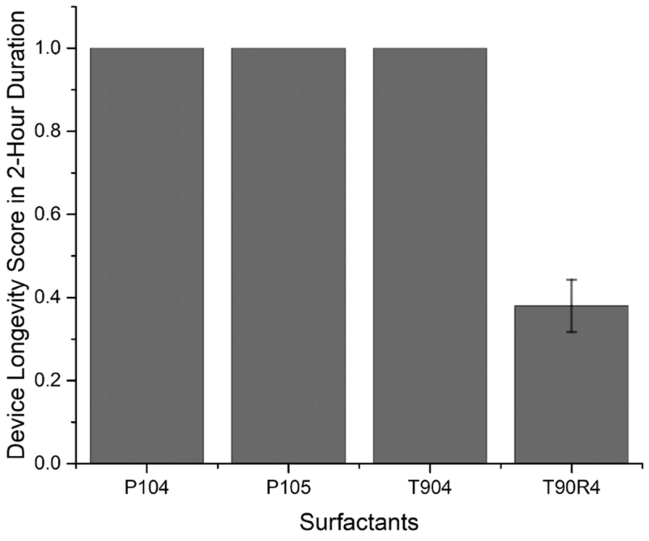


**Figure 4.** Two-hour device longevity assay results. Plot of device longevity scores for 0.1% wt/wt surfactants P104, P105, T904, and T90R4 in 90% v/v fetal bovine serum. Error bars represent ±1 std. deviation of the longevity score for $n$ = 3 replicate droplets per condition. No error bars are indicated for the conditions that had perfect scores in all of the replicates.

BSA and four concentrations of five different surfactants) were formed and tested. As shown in Table 2, the minimum concentration of one surfactant, F68, scaled with [BSA], requiring high surfactant concentration for droplet actuation at high BSA concentration. In contrast, the minimum concentrations of the other surfactants, P104, P105, T904, and T90R4, were independent of BSA concentration. While these results are not conclusive on their own, they are consistent with F68 potentially preventing fouling by forming a complex with BSA, and P104, P105, T904, and T90R4 potentially not relying on complexation with BSA under these conditions.

As a second test for the antifouling mechanism of Pluronic/Tetronic surfactant additives in DMF, we used orthogonal methods to probe for surfactant−protein complexation, including intrinsic fluorescence, dynamic light scattering (DLS), and asymmetric flow field flow fractionation with multiangle light scattering ($AF_4$-MLS). Intrinsic fluorescence evaluates emission from Trp-134 and Trp-212 residues[64] in BSA, which is highly sensitive to the local chemical environment, and can report structural changes,[64] potentially including those caused by complexation with surfactants. Typical results are shown in Figure 5a—as indicated, solutions of BSA alone and BSA mixed with each of the Pluronic/Tetronic surfactants at the minimum concentration needed to manipulate this sample (from Table 2) exhibit intrinsic fluorescence at maxima of around 350 nm. In contrast, for BSA mixed with SDS (as a positive control, known to interact and complex with BSA[65]), the fluorescence maximum is blue-shifted to around 320 nm. Results generated using DLS and $AF_4$-MLS (Figure 5b and Table 3) tell a similar story; with average hydrodynamic diameter and average molecular weight for BSA alone (9.66 nm and 6.80 × $10^4$ g/mol, respectively) being similar to the measurements found for BSA mixed with Pluronic/Tetronic additives. In contrast, BSA mixed with SDS yielded values (11.8 nm and 7.55 × $10^4$ g/mol, respectively) that were 10−20% greater than BSA alone, suggesting complexation. Taken


https://doi.org/10.1021/acsami.2c17317
ACS Appl. Mater. Interfaces 2023, 15, 6326−6337

**Table 2. Minimum Concentration of Pluronic and Tetronic Additives Enabling High-Longevity DMF Actuation of BSA**

| surfactant additive | minimum surfactant concentration (% wt/wt) enabling droplet movement with longevity score = 1.00 for 10 min of continuous actuation ($n$ = 3) | | |
|---|---|---|---|
| | 40 mg/mL (0.600 mM) BSA | 4 mg/mL (0.060 mM) BSA | 0.4 mg/mL (0.006 mM) BSA |
| F68 | 2.0% (2.00 mM) | 0.10% (0.10 mM) | 0.10% (0.10 mM) |
| P104 | 0.01% (0.02 mM) | 0.01% (0.02 mM) | 0.01% (0.02 mM) |
| P105 | 0.01% (0.02 mM) | 0.01% (0.02 mM) | 0.01% (0.02 mM) |
| T904 | 0.01% (0.01 mM) | 0.01% (0.01 mM) | 0.01% (0.01 mM) |
| T90R4 | 0.01% (0.01 mM) | 0.01% (0.01 mM) | 0.01% (0.01 mM) |

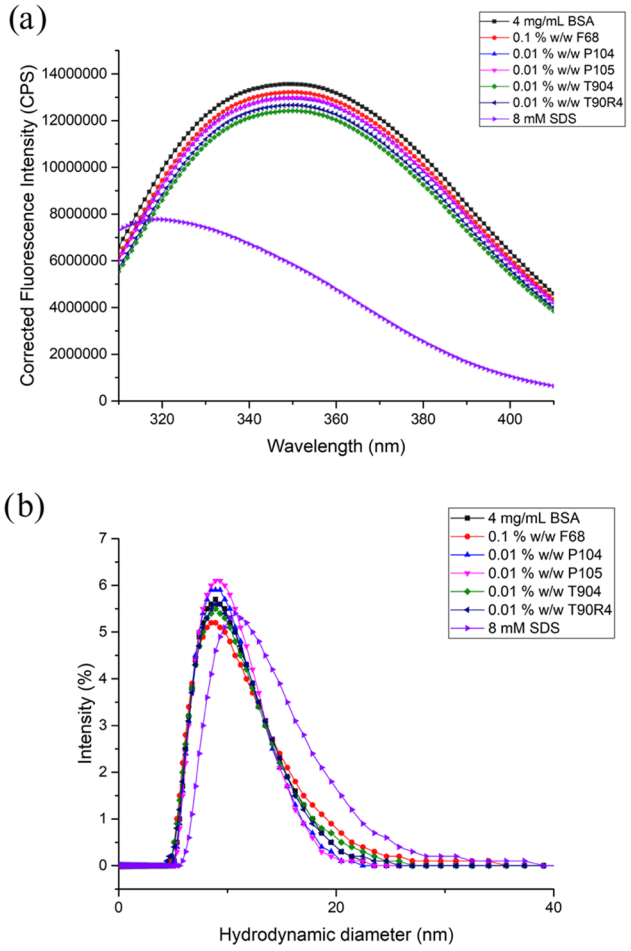


**Figure 5.** BSA complexation experiments. (a) Intrinsic fluorescence spectra for BSA with and without surfactants. (b) Dynamic light scattering plot of hydrodynamic diameter of BSA with and without surfactants. In both datasets, samples include 4 mg/mL BSA in DPBS (black squares), or in DPBS containing Pluronics (F68, 0.1%—red circles, P104, 0.01%—blue triangles, P105, 0.01%—pink inverted triangles), Tetronics (904, 0.01%—green diamonds, 90R4, 0.01%—dark blue left-pointing triangles), or SDS (8 mM—violet right-pointing triangles).

together, these results support a hypothesis that the Pluronic/Tetronic additives under the conditions evaluated here do not form noticeable complexes with BSA.

As a third test for the antifouling mechanism of Pluronic/Tetronic surfactant additives in DMF, we used the emerging technique of supercritical angle fluorescence (SAF) microscopy[50] to probe for potential interactions between fluorescently labeled surfactants and fluoropolymer-coated surfaces. (As illustrated in Figure S3, SAF microscopy allows for discrimination between fluorophores in bulk solution and those

**Table 3. Mean Hydrodynamic Diameter (by DLS), Average Molecular Mass (by $AF_4$), and Range of Molecular Masses (by $AF_4$) of BSA in Pluronic and Tetronic Additives**

| surfactant additive and concentration | mean hydrodynamic diameter of BSA ± 1 SD (nm) | average molecular mass ($\times 10^4$ g/mol) | range of ave. mol. mass ($\times 10^4$ g/mol) |
|---|---|---|---|
| no surfactant | 9.6 ± 0.1 | 6.80 | 5.74−8.12 |
| 0.10% wt/wt F68 | 9.5 ± 0.1 | 6.31 | 4.73−7.90 |
| 0.01% wt/wt P104 | 9.5 ± 0.2 | 6.47 | 4.99−7.96 |
| 0.01% wt/wt P105 | 9.5 ± 0.1 | 6.41 | 4.92−7.91 |
| 0.01% wt/wt T904 | 9.5 ± 0.2 | 6.26 | 5.10−7.42 |
| 0.01% wt/wt T90R4 | 9.4 ± 0.1 | 6.49 | 5.04−7.94 |
| 8 mM SDS | 12.0 ± 0.1 | 7.55 | 5.69−9.41 |

adsorbed on surfaces.[66,67]) A method was adapted from Ahmed et al.[48] to label Pluronic/Tetronic surfactants with the fluorescein derivative 5-DTAF, which was confirmed to be successful for F68, P105, and T904 by absorbance spectroscopy (Figure S4). A colorimetric assay adapted from Ghebeh et al.[49] was used to determine the concentration of the labeled surfactants after labeling and cleanup (using the calibration curves in Figure S5), and labeling efficiency was determined using a calibration curve of free 5-DTAF (Figure S6). The interactions of labeled surfactants with Teflon-AF-coated glass surfaces (proxies for DMF devices) were then monitored by SAF microscopy. As a control, solutions containing similar amounts of free fluorescein (30 $\mu$M) to the concentration of fluorophores in the labeled surfactant solutions (Table S2) were formed in unlabeled surfactant solutions. Excitation intensities were adjusted to match the subcritical intensity of each labeled surfactant with its control solution, preventing over-estimation of SAF signal and minimizing the "bleed-through effect" from the subcritical region.[50] Representative images are shown in Figure 6a,b; as shown, labeled surfactants exhibited the classic "ring" shape associated with surface association, while controls did not. Quantified SAF signals are given in Figure 6c (Table S3, columns 2−3)—as indicated, all of the labeled surfactants have SAF signals that are greater than their respective controls by at least a factor of 10, which suggests preferential adsorption of labeled surfactants at the fluoropolymer surface. With the presence of high concentrations of BSA (Figure 6d and Table S3, columns 4−5), the SAF signal of the surfaces exposed to labeled surfactants remained higher than the control by at least a factor of 3. Taken together, these results suggest that F68, P105, and T904 may potentially resist protein adsorption by forming a "protective layer" on the Teflon surface. These results are compelling but not (on their own) conclusive, given the unknown effects of the fluorescent labels on the behavior of the surfactants.


https://doi.org/10.1021/acsami.2c17317
ACS Appl. Mater. Interfaces 2023, 15, 6326−6337

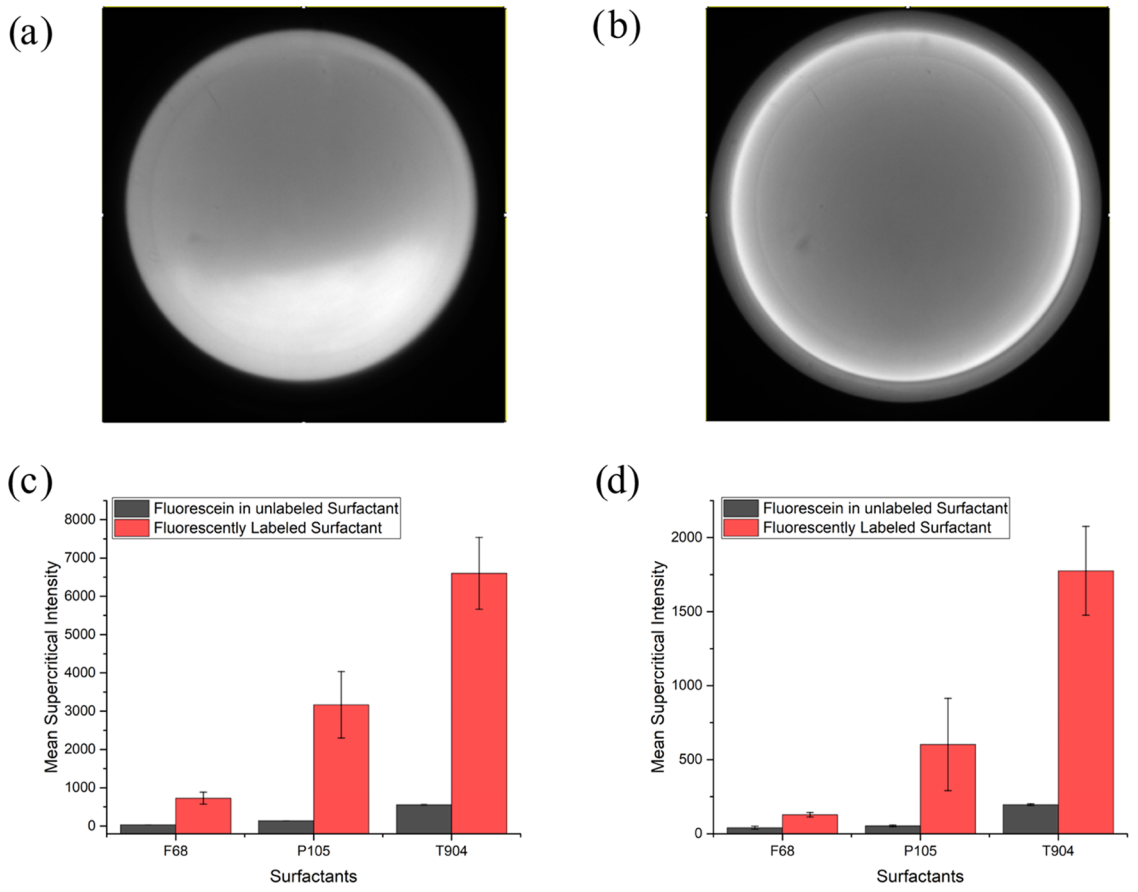


**Figure 6.** Surface adsorption measurements. Representative SAF images of (a) 30 $\mu$M fluorescein in 0.1% wt/wt T904 in DPBS and (b) 0.1% wt/wt 5-DTAF labeled T904 in DPBS. Plots of mean supercritical fluorescence (SAF) emission of 30 $\mu$M fluorescein in 0.1% wt/wt unlabeled surfactant (black) and 0.1% wt/wt 5-DTAF labeled surfactants (red) in (c) DPBS and in (d) 40 mg/mL BSA in DPBS on Teflon-AF-coated cover glasses. Error bars are ± 1 std. dev. of for $n$ = 5 replicate droplets per condition.

As a fourth (and final) test for the antifouling mechanism of Pluronic/Tetronic surfactant additives in DMF, we used two orthogonal techniques to probe for potential interactions between native (unlabeled) surfactants and fluoropolymer-coated surfaces: atomic force microscopy (AFM) and quartz crystal microbalance with dissipation (QCM-D) monitoring. AFM images of Teflon-AF surfaces immersed in buffer alone, buffer with F68, buffer with T904 are shown in Figure S7. Roughness data extracted from these measurements (Table S4) indicate substantially greater roughness for surfaces exposed to surfactants, consistent with the formation of a layer of surfactant at the interface. Likewise, Teflon-AF-coated QCM-D sensors reported an increase in mass when exposed to solutions of F68 or T904, with magnitudes that are greater than what is observed from a solution of PEG 8000 (a similarly sized solute expected to not interact with the surface) (Figure S8). Taken together, these data are also consistent with the formation of surface-adsorbed layers of Pluronic or Tetronic on Teflon-AF.

The results described above show little evidence that Pluronic or Tetronic additives form complexes with proteins and substantial evidence that they adsorb to the fluoropolymer–liquid interface in DMF. The latter is consistent with literature reports that Pluronics and Tetronics adsorb to hydrophobic surfaces.[68,69] DMF is unique in that this effect is presumably transient during droplet translation, forming at a given spot when a droplet first crosses it, and then disassembling rapidly as the droplet leaves that (now-dry) spot behind; we propose that SAF microscopy may be a useful technique to study this presumption in the future. Regardless of the mechanism, these findings are consistent with hypothesis (ii) from the introduction—that Pluronic and Tetronic additives resist fouling in DMF by forming a protective coating on device surfaces, preventing protein adsorption.

## CONCLUSIONS

We evaluated 19 Pluronic and Tetronic surfactants as additives for reducing protein adsorption in digital microfluidics. Among all of the surfactants tested, Pluronic P104 and P105, and Tetronic 904 showed exceptional antifouling performance, allowing for continuous actuation in DMF devices for over 2 h. All of these surfactants have modest mass, PPO content of ≥50 units, PEO mass % ≤50%, and HLB value between 13 and 15. Additional experiments relying on device longevity measurements, intrinsic fluorescence, DLS, $AF_4$-MLS, SAF microscopy, AFM, and QCM-D measurements suggest that Pluronics and Tetronics act to prevent surface fouling through forming a protective layer at the fluoropolymer device surface, rather than by forming surfactant–protein complexes.

## ASSOCIATED CONTENT

### Supporting Information

The Supporting Information is available free of charge at https://pubs.acs.org/doi/10.1021/acsami.2c17317.



https://doi.org/10.1021/acsami.2c17317
ACS Appl. Mater. Interfaces 2023, 15, 6326–6337

Representative force−velocity plots (Figure S1), CMC determination data (Figure S2), supercritical fluorescence data (Figure S3), surfactant derivatization data (Figure S4), calibration curves for quantification of surfactants (Figure S5), calibration curve for quantification of derivatized fraction of surfactants (Figure S6), representative atomic force microscopy images (Figure S7), representative QCM-D data (Figure S8), comprehensive device longevity test results (Table S1), conjugation efficiency data (Table S2), supercritical fluorescence intensity data (Table S3), and surface roughness data (Table S4) (PDF)

Representative video clips (at 8× frame rate) of droplets undergoing a device longevity test, including a fluid with perfect longevity (fetal bovine serum with 0.35% wt/wt T904, green), a fluid with poor longevity (fetal bovine serum with 2.0% wt/wt L62, yellow), and a fluid that is immobile (fetal bovine serum, red); food coloring dyes were added to the droplets for visualization (Movie S1) (MP4)

## AUTHOR INFORMATION


### Corresponding Author

**Aaron R. Wheeler** − *Department of Chemistry, University of Toronto, Toronto, Ontario M5S 3H6, Canada; Donnelly Centre for Cellular and Biomolecular Research, University of Toronto, Toronto, Ontario M5S 3E1, Canada; Institute of Biomedical Engineering, University of Toronto, Toronto, Ontario M5S 3G9, Canada;* orcid.org/0000-0001-5230-7475; Email: aaron.wheeler@utoronto.ca

### Authors

**Man Ho** − *Department of Chemistry, University of Toronto, Toronto, Ontario M5S 3H6, Canada; Donnelly Centre for Cellular and Biomolecular Research, University of Toronto, Toronto, Ontario M5S 3E1, Canada*

**Aaron Au** − *Donnelly Centre for Cellular and Biomolecular Research, University of Toronto, Toronto, Ontario M5S 3E1, Canada; Institute of Biomedical Engineering, University of Toronto, Toronto, Ontario M5S 3G9, Canada*

**Robert Flick** − *Department of Chemical Engineering & Applied Chemistry, University of Toronto, Toronto, Ontario M5S 3E5, Canada;* orcid.org/0000-0001-5463-9107

**Thu V. Vuong** − *Department of Chemical Engineering & Applied Chemistry, University of Toronto, Toronto, Ontario M5S 3E5, Canada*

**Alexandros A. Sklavounos** − *Department of Chemistry, University of Toronto, Toronto, Ontario M5S 3H6, Canada; Donnelly Centre for Cellular and Biomolecular Research, University of Toronto, Toronto, Ontario M5S 3E1, Canada;* orcid.org/0000-0003-1495-7156

**Ian Swyer** − *Department of Chemistry, University of Toronto, Toronto, Ontario M5S 3H6, Canada*

**Christopher M. Yip** − *Donnelly Centre for Cellular and Biomolecular Research, University of Toronto, Toronto, Ontario M5S 3E1, Canada; Institute of Biomedical Engineering, University of Toronto, Toronto, Ontario M5S 3G9, Canada; Department of Chemical Engineering & Applied Chemistry, University of Toronto, Toronto, Ontario M5S 3E5, Canada; Department of Biochemistry, University of Toronto, Toronto, Ontario M5S 1A8, Canada;* orcid.org/0000-0003-4507-556X

Complete contact information is available at: https://pubs.acs.org/10.1021/acsami.2c17317


### Author Contributions

M.H., I.S., and A.R.W. conceived of the idea for standardizing device longevity assays based on threshold force and minimum velocity threshold. I.S. and A.A.S. wrote the Python code for droplet movement analysis and data extraction from MicroDrop. M.H. conducted all surfactant screening, longevity tests, surfactant−protein characterization (DLS, UV−vis), and associated data analysis. R.F. and T.V.V. conducted $AF_4$ and QCM-D data collection and analysis, respectively, in the U of T BioZone facility. A.A. and M.H. conceived of the idea for monitoring fluorescently labeled surfactant adsorption on a thin-film Teflon-AF using supercritical fluorescence angle microscopy. All reagents, micro-cover glass slides, and Teflon-AF coating used in supercritical fluorescence angle measurements were prepared by M.H. in the A.R.W. Lab. All SAF experiments were performed by A.A. and M.H. in the C.M.Y. Lab. The SAF microscope was built and optimized, as well as SAF data were analyzed by A.A. in the C.M.Y. Lab. M.H. and A.R.W. interpreted results and wrote the manuscript with contributions from all authors.

### Notes

The authors declare the following competing financial interest(s): M.H. and A.R.W are co-inventors on a patent (US 11,292,002 B2) that describes some of the anti-fouling strategies for digital microfluidics that are described here.

## ACKNOWLEDGMENTS

The authors thank Dr. Vivienne Luk and Dr. Sam Au for laying the groundwork for probing the effects of Pluronic additives in DMF, and Dr. Ryan Fobel and Dr. Alphonsus Ng for bringing Tetronic additives into the story. They thank Prof. Walid Houry, Dr. Thiago Vargas Seraphim, Prof. Edgar Acosta, and Prof. Wihelm Neumann for insightful discussions about proteins, surfactants, complexation, and surface tension. They also acknowledge Prof. Gilbert Walker, Prof. Warren Chan, Prof. Molly Shoichet, Dr. Wei Qing, Wayne Ngo, and Matthew Nguyen for providing access to and training on many of the instruments used herein (i.e., DLS, AFM, Fluorimeter, UV−vis spectrometer, and plate reader). Finally, the authors acknowledge support from the Natural Sciences and Engineering Research Council of Canada (C.M.Y.: RGPIN-2022-048; A.R.W.: RGPIN 2019-04867).

## REFERENCES


(1) Harding, J. L.; Reynolds, M. M. Combating Medical Device Fouling. *Trends Biotechnol.* **2014**, *32*, 140−146.

(2) Thevenot, P.; Hu, W.; Tang, L. Surface Chemistry Influences Implant Biocompatibility. *Curr. Top. Med. Chem.* **2008**, *8*, 270−280.

(3) Meng, F.; Zhang, S.; Oh, Y.; Zhou, Z.; Shin, H.-S.; Chae, S.-R. Fouling in Membrane Bioreactors: An Updated Review. *Water Res.* **2017**, *114*, 151−180.

(4) Amy, G. Fundamental Understanding of Organic Matter Fouling of Membranes. *Desalination* **2008**, *231*, 44−51.

(5) Nguyen, T.; Roddick, F. A.; Fan, L. Biofouling of Water Treatment Membranes: A Review of the Underlying Causes, Monitoring Techniques and Control Measures. *Membranes* **2012**, *2*, 804−840.

(6) Boardman, A. K.; Allison, S.; Sharon, A.; Sauer-Budge, A. F. Comparison of Anti-Fouling Surface Coatings for Applications in Bacteremia Diagnostics. *Anal. Methods* **2013**, *5*, 273−280.

(7) Zhang, H.; Chiao, M. Anti-Fouling Coatings of Poly-(Dimethylsiloxane) Devices for Biological and Biomedical Applications. *J. Med. Biol. Eng.* **2015**, *35*, 143−155.
(8) Wang, R. L. C.; Kreuzer, H. J.; Grunze, M. Molecular Conformation and Solvation of Oligo(Ethylene Glycol)-Terminated Self-Assembled Monolayers and Their Resistance to Protein Adsorption. *J. Phys. Chem. B* **1997**, *101*, 9767−9773.
(9) Amiji, M.; Park, K. Prevention of Protein Adsorption and Platelet Adhesion on Surfaces by PEO/PPO/PEO Triblock Copolymers. *Biomaterials* **1992**, *13*, 682−692.
(10) Ebara, M.; Hoffman, J. M.; Stayton, P. S.; Hoffman, A. S. Surface Modification of Microfluidic Channels by Uv-Mediated Graft Polymerization of Non-Fouling and 'Smart' Polymers. *Radiat. Phys. Chem.* **2007**, *76*, 1409−1413.
(11) Guo, D.-J.; Han, H.-M.; Jing, W.; Xiao, S.-J.; Dai, Z.-D. Surface-Hydrophilic and Protein-Resistant Silicone Elastomers Prepared by Hydrosilylation of Vinyl Poly(Ethylene Glycol) on Hydrosilanes-Poly(Dimethylsiloxane) Surfaces. *Colloids Surf., A* **2007**, *308*, 129−135.
(12) Choi, K.; Ng, A. H.; Fobel, R.; Wheeler, A. R. Digital Microfluidics. *Annu. Rev. Anal. Chem.* **2012**, *5*, 413−440.
(13) Wang, H.; Chen, L.; Sun, L. Digital Microfluidics: A Promising Technique for Biochemical Applications. *Front. Mech. Eng.* **2017**, *12*, 510−525.
(14) Lamanna, J.; Scott, E. Y.; Edwards, H. S.; Chamberlain, M. D.; Dryden, M. D. M.; Peng, J.; Mair, B.; Lee, A.; Chan, C.; Sklavounos, A. A.; Heffernan, A.; Abbas, F.; Lam, C.; Olson, M. E.; Moffat, J.; Wheeler, A. R. Digital Microfluidic Isolation of Single Cells for Omics. *Nat. Commun.* **2020**, *11*, No. 5632.
(15) Ruan, Q.; Ruan, W.; Lin, X.; Wang, Y.; Zou, F.; Zhou, L.; Zhu, Z.; Yang, C. Digital-Wgs: Automated, Highly Efficient Whole-Genome Sequencing of Single Cells by Digital Microfluidics. *Sci. Adv.* **2020**, *6*, No. eabd6454.
(16) Sklavounos, A. A.; Nemr, C. R.; Kelley, S. O.; Wheeler, A. R. Bacterial Classification and Antibiotic Susceptibility Testing on an Integrated Microfluidic Platform. *Lab Chip* **2021**, *21*, 4208−4222.
(17) Qiu, W.; Nagl, S. Automated Miniaturized Digital Microfluidic Antimicrobial Susceptibility Test Using a Chip-Integrated Optical Oxygen Sensor. *ACS Sens.* **2021**, *6*, 1147−1156.
(18) Coudron, L.; McDonnell, M. B.; Munro, I.; McCluskey, D. K.; Johnston, I. D.; Tan, C. K. L.; Tracey, M. C. Fully Integrated Digital Microfluidics Platform for Automated Immunoassay; a Versatile Tool for Rapid, Specific Detection of a Wide Range of Pathogens. *Biosens. Bioelectron.* **2019**, *128*, 52−60.
(19) de Campos, R. P. S.; Rackus, D. G.; Shih, R.; Zhao, C.; Liu, X.; Wheeler, A. R. "Plug-N-Play" Sensing with Digital Microfluidics. *Anal. Chem.* **2019**, *91*, 2506−2515.
(20) Latip, E. N. A.; Coudron, L.; McDonnell, M. B.; Johnston, I. D.; McCluskey, D. K.; Day, R.; Tracey, M. C. Protein Droplet Actuation on Superhydrophobic Surfaces: A New Approach toward Anti-Biofouling Electrowetting Systems. *RSC Adv.* **2017**, *7*, 49633−49648.
(21) Yoon, J.-Y.; Garrell, R. L. Preventing Biomolecular Adsorption in Electrowetting-Based Biofluidic Chips. *Anal. Chem.* **2003**, *75*, 5097−5102.
(22) Geng, H.; Cho, S. K. Antifouling Digital Microfluidics Using Lubricant Infused Porous Film. *Lab Chip* **2019**, *19*, 2275−2283.
(23) Freire, S. L. S.; Tanner, B. Additive-Free Digital Microfluidics. *Langmuir* **2013**, *29*, 9024−9030.
(24) Au, S. H.; Kumar, P.; Wheeler, A. R.; New, A. Angle on Pluronic Additives: Advancing Droplets and Understanding in Digital Microfluidics. *Langmuir* **2011**, *27*, 8586−8594.
(25) Luk, V. N.; Mo, G.; Wheeler, A. R. Pluronic Additives: A Solution to Sticky Problems in Digital Microfluidics. *Langmuir* **2008**, *24*, 6382−6389.
(26) Kühnemund, M.; Witters, D.; Nilsson, M.; Lammertyn, J. Circle-to-Circle Amplification on a Digital Microfluidic Chip for Amplified Single Molecule Detection. *Lab Chip* **2014**, *14*, 2983−2992.
(27) Piao, Y.; Wang, X.; Xia, H.; Wang, W. Digital Microfluidic Platform for Automated Detection of Human Chorionic Gonadotropin. *Microfluid. Nanofluid.* **2019**, *23*, 1.
(28) Gach, P. C.; Shih, S. C. C.; Sustarich, J.; Keasling, J. D.; Hillson, N. J.; Adams, P. D.; Singh, A. K. A Droplet Microfluidic Platform for Automating Genetic Engineering. *ACS Synth. Biol.* **2016**, *5*, 426−433.
(29) Wang, Y.; Ruan, Q.; Lei, Z.-C.; Lin, S.-C.; Zhu, Z.; Zhou, L.; Yang, C. Highly Sensitive and Automated Surface Enhanced Raman Scattering-Based Immunoassay for H5N1 Detection with Digital Microfluidics. *Anal. Chem.* **2018**, *90*, 5224−5231.
(30) Witters, D.; Knez, K.; Ceyssens, F.; Puers, R.; Lammertyn, J. Digital Microfluidics-Enabled Single-Molecule Detection by Printing and Sealing Single Magnetic Beads in Femtoliter Droplets. *Lab Chip* **2013**, *13*, 2047−2054.
(31) Huang, H.-Y.; Shen, H.-H.; Tien, C.-H.; Li, C.-J.; Fan, S.-K.; Liu, C.-H.; Hsu, W.-S.; Yao, D.-J. Digital Microfluidic Dynamic Culture of Mammalian Embryos on an Electrowetting on Dielectric (EWOD) Chip. *PLoS One* **2015**, *10*, No. e0124196.
(32) Nelson, W. C.; Peng, I.; Lee, G.-A.; Loo, J. A.; Garrell, R. L.; Cj Kim, C.-J. Incubated Protein Reduction and Digestion on an Electrowetting-on-Dielectric Digital Microfluidic Chip for MALDI-MS. *Anal. Chem.* **2010**, *82*, 9932−9937.
(33) Park, S.; Wijethunga, P. A. L.; Moon, H.; Han, B. On-Chip Characterization of Cryoprotective Agent Mixtures Using an EWOD-Based Digital Microfluidic Device. *Lab Chip* **2011**, *11*, 2212−2221.
(34) Huang, H.-Y.; Shen, H.; Chung, L.; Chung, Y.; Chen, C.; Hsu, C.; Fan, S.; Yao, D. Fertilization of Mouse Gametes in Vitro Using a Digital Microfluidic System. *IEEE Trans. Nanobiosci.* **2015**, *14*, 857−863.
(35) Lee, M.-S.; Hsu, W.; Huang, H.-Y.; Tseng, H.-Y.; Lee, C.-T.; Hsu, C.-Y.; Shieh, Y.-C.; Wang, S.-H.; Yao, D.-J.; Liu, C.-H. Simultaneous Detection of Two Growth Factors from Human Single-Embryo Culture Medium by a Bead-Based Digital Microfluidic Chip. *Biosens. Bioelectron.* **2020**, *150*, No. 111851.
(36) Sathyanarayanan, G.; Haapala, M.; Sikanen, T. Digital Microfluidics-Enabled Analysis of Individual Variation in Liver Cytochrome P450 Activity. *Anal. Chem.* **2020**, *92*, 14693−14701.
(37) Seale, B.; Lam, C.; Rackus, D. G.; Chamberlain, M. D.; Liu, C.; Wheeler, A. R. Digital Microfluidics for Immunoprecipitation. *Anal. Chem.* **2016**, *88*, 10223−10230.
(38) Ng, A. H. C.; Fobel, R.; Fobel, C.; Lamanna, J.; Rackus, D. G.; Summers, A.; Dixon, C.; Dryden, M. D. M.; Lam, C.; Ho, M.; Mufti, N. S.; Lee, V.; Asri, M. A. M.; Sykes, E. A.; Chamberlain, M. D.; Joseph, R.; Ope, M.; Scobie, H. M.; Knipes, A.; Rota, P. A.; Marano, N.; Chege, P. M.; Njuguna, M.; Nzunza, R.; Kisangau, N.; Kiogora, J.; Karuingi, M.; Burton, J. W.; Borus, P.; Lam, E.; Wheeler, A. R. A Digital Microfluidic System for Serological Immunoassays in Remote Settings. *Sci. Transl. Med.* **2018**, *10*, No. eaar6076.
(39) Sklavounos, A. A.; Lamanna, J.; Modi, D.; Gupta, S.; Mariakakis, A.; Callum, J.; Wheeler, A. R. Digital Microfluidic Hemagglutination Assays for Blood Typing, Donor Compatibility Testing, and Hematocrit Analysis. *Clin. Chem.* **2021**, *67*, 1699−1708.
(40) Dixon, C.; Lamanna, J.; Wheeler, A. R. Direct Loading of Blood for Plasma Separation and Diagnostic Assays on a Digital Microfluidic Device. *Lab Chip* **2020**, *20*, 1845−1855.
(41) Ottenbrite, R. M.; Javan, R. Biological Structures. In *Encyclopedia of Condensed Matter Physics*, Bassani, F.; Liedl, G. L.; Wyder, P., Eds.; Elsevier: Oxford, 2005; pp 99−108.
(42) Chen, Y.; Liu, T.; Xu, G.; Zhang, J.; Zhai, X.; Yuan, J.; Tan, Y. Aggregation Behavior of X-Shaped Branched Block Copolymers at the Air/Water Interface: Effect of Block Sequence and Temperature. *Colloid Polym. Sci.* **2015**, *293*, 97−107.
(43) Lee, H. J.; McAuley, A.; Schilke, K. F.; McGuire, J. Molecular Origins of Surfactant-Mediated Stabilization of Protein Drugs. *Adv. Drug Delivery Rev.* **2011**, *63*, 1160−1171.
(44) Jia, Y.; Narayanan, J.; Liu, X.-Y.; Liu, Y. Investigation on the Mechanism of Crystallization of Soluble Protein in the Presence of Nonionic Surfactant. *Biophys. J.* **2005**, *89*, 4245−4251.
(45) Dixon, C.; Ng, A. H. C.; Fobel, R.; Miltenburg, M. B.; Wheeler, A. R. An Inkjet Printed, Roll-Coated Digital Microfluidic Device for Inexpensive, Miniaturized Diagnostic Assays. *Lab Chip* **2016**, *16*, 4560−4568.


https://doi.org/10.1021/acsami.2c17317
*ACS Appl. Mater. Interfaces* 2023, 15, 6326−6337

(46) Swyer, I.; Fobel, R.; Wheeler, A. R. Velocity Saturation in Digital Microfluidics. *Langmuir* **2019**, *35*, 5342−5352.
(47) Fobel, R.; Fobel, C.; Wheeler, A. Dropbot: An Open-Source Digital Microfluidic Control System with Precise Control of Electrostatic Driving Force and Instantaneous Drop Velocity Measurement. *Appl. Phys. Lett.* **2013**, *102*, No. 193513.
(48) Ahmed, F.; Alexandridis, P.; Neelamegham, S. Synthesis and Application of Fluorescein-Labeled Pluronic Block Copolymers to the Study of Polymer−Surface Interactions. *Langmuir* **2001**, *17*, 537−546.
(49) Ghebeh, H.; Handa-Corrigan, A.; Butler, M. Development of an Assay for the Measurement of the Surfactant Pluronic F-68 in Mammalian Cell Culture Medium. *Anal. Biochem.* **1998**, *262*, 39−44.
(50) Au, A.; Ho, M.; Wheeler, A. R.; Yip, C. M. Monitoring Non-Specific Adsorption at Solid−Liquid Interfaces by Supercritical Angle Fluorescence Microscopy. *Rev. Sci. Instrum.* **2022**, *93*, No. 113707.
(51) Edelstein, A. D.; Tsuchida, M. A.; Amodaj, N.; Pinkard, H.; Vale, R. D.; Stuurman, N. Advanced Methods of Microscope Control Using Mmanager Software. *J. Biol. Methods* **2014**, *1*, No. e10.
(52) Voinova, M. V.; Rodahl, M.; Jonson, M.; Kasemo, B. Viscoelastic Acoustic Response of Layered Polymer Films at Fluid-Solid Interfaces: Continuum Mechanics Approach. *Phys. Scr.* **1999**, *59*, 391.
(53) Alvarez-Lorenzo, C.; Rey-Rico, A.; Sosnik, A.; Taboada, P.; Concheiro, A. Poloxamine-Based Nanomaterials for Drug Delivery. *Front. Biosci.* **2010**, *E2*, 424−440.
(54) Alvarez-Lorenzo, C.; Sosnik, A.; Concheiro, A. PEO-PPO Block Copolymers for Passive Micellar Targeting and Overcoming Multidrug Resistance in Cancer Therapy. *Curr. Drug Targets* **2011**, *12*, 1112−1130.
(55) Batrakova, E.; Lee, S.; Li, S.; Venne, A.; Alakhov, V.; Kabanov, A. Fundamental Relationships between the Composition of Pluronic Block Copolymers and Their Hypersensitization Effect in Mdr Cancer Cells. *Pharm. Res.* **1999**, *16*, 1373−1379.
(56) Green, R. J.; Davies, M. C.; Roberts, C. J.; Tendler, S. J. A Surface Plasmon Resonance Study of Albumin Adsorption to PEO-PPO-PEO Triblock Copolymers. *J. Biomed. Mater. Res.* **1998**, *42*, 165−171.
(57) Fluksman, A.; Benny, O.; Robust, A. Method for Critical Micelle Concentration Determination Using Coumarin-6 as a Fluorescent Probe. *Anal. Methods* **2019**, *11*, 3810−3818.
(58) Jin, K.; Hu, C.; Hu, S.; Hu, C.; Li, J.; Ma, H. "One-to-Three" Droplet Generation in Digital Microfluidics for Parallel Chemiluminescence Immunoassays. *Lab Chip* **2021**, *21*, 2892−2900.
(59) Leipert, J.; Steinbach, M. K.; Tholey, A. Isobaric Peptide Labeling on Digital Microfluidics for Quantitative Low Cell Number Proteomics. *Anal. Chem.* **2021**, *93*, 6278−6286.
(60) Garidel, P.; Hoffmann, C.; Blume, A. A Thermodynamic Analysis of the Binding Interaction between Polysorbate 20 and 80 with Human Serum Albumins and Immunoglobulins: A Contribution to Understand Colloidal Protein Stabilisation. *Biophys. Chem.* **2009**, *143*, 70−78.
(61) Mollmann, S. H.; Elofsson, U.; Bukrinsky, J. T.; Frokjaer, S. Displacement of Adsorbed Insulin by Tween 80 Monitored Using Total Internal Reflection Fluorescence and Ellipsometry. *Pharm. Res.* **2005**, *22*, 1931−1941.
(62) Zadymova, N. M.; Yampol'skaya, G. P.; Filatova, L. Y. Interaction of Bovine Serum Albumin with Nonionic Surfactant Tween 80 in Aqueous Solutions: Complexation and Association. *Colloid J.* **2006**, *68*, 162−172.
(63) Gelamo, E. L.; Silva, C. H. T. P.; Imasato, H.; Tabak, M. Interaction of Bovine (BSA) and Human (HSA) Serum Albumins with Ionic Surfactants: Spectroscopy and Modelling. *Biochim. Biophys. Acta, Protein Struct. Mol. Enzymol.* **2002**, *1594*, 84−99.
(64) Lu, R.-C.; Cao, A.-N.; Lai, L.-H.; Xiao, J.-X. Effect of Anionic Surfactant Molecular Structure on Bovine Serum Albumin (BSA) Fluorescence. *Colloids Surf., A* **2006**, *278*, 67−73.
(65) Santos, S. F.; Zanette, D.; Fischer, H.; Itri, R.; Systematic, A. Study of Bovine Serum Albumin (BSA) and Sodium Dodecyl Sulfate (SDS) Interactions by Surface Tension and Small Angle X-Ray Scattering. *J. Colloid Interface Sci.* **2003**, *262*, 400−408.
(66) Ries, J.; Ruckstuhl, T.; Verdes, D.; Schwille, P. Supercritical Angle Fluorescence Correlation Spectroscopy. *Biophys. J.* **2008**, *94*, 221−229.
(67) Dasgupta, A.; Deschamps, J.; Matti, U.; Hübner, U.; Becker, J.; Strauss, S.; Jungmann, R.; Heintzmann, R.; Ries, J. Direct Supercritical Angle Localization Microscopy for Nanometer 3d Superresolution. *Nat. Commun.* **2021**, *12*, No. 1180.
(68) Nejadnik, M. R.; Olsson, A. L. J.; Sharma, P. K.; van der Mei, H. C.; Norde, W.; Busscher, H. J. Adsorption of Pluronic F-127 on Surfaces with Different Hydrophobicities Probed by Quartz Crystal Microbalance with Dissipation. *Langmuir* **2009**, *25*, 6245−6249.
(69) Song, X.; Zhao, S.; Fang, S.; Ma, Y.; Duan, M. Mesoscopic Simulations of Adsorption and Association of PEO-PPO-PEO Triblock Copolymers on a Hydrophobic Surface: From Mushroom Hemisphere to Rectangle Brush. *Langmuir* **2016**, *32*, 11375−11385.


https://doi.org/10.1021/acsami.2c17317
*ACS Appl. Mater. Interfaces* 2023, 15, 6326−6337